

HST/STIS ULTRAVIOLET IMAGING OF POLAR AURORA ON GANYMEDE

PAUL D. FELDMAN,¹ MELISSA A. MCGRATH,² DARRELL F. STROBEL,^{1,3} H. WARREN MOOS,¹
KURT D. RETHERFORD,¹ AND BRIAN C. WOLVEN¹

Accepted for publication in the Astrophysical Journal

ABSTRACT

We report new observations of the spectrum of Ganymede in the spectral range 1160 – 1720 Å made with the Space Telescope Imaging Spectrograph (STIS) on HST on 1998 October 30. The observations were undertaken to locate the regions of the atomic oxygen emissions at 1304 and 1356 Å, previously observed with the Goddard High Resolution Spectrograph on HST, that Hall et al. (1998) claimed indicated the presence of polar aurorae on Ganymede. The use of the 2'' wide STIS slit, slightly wider than the disk diameter of Ganymede, produced objective spectra with images of the two oxygen emissions clearly separated. The O I emissions appear in both hemispheres, at latitudes above 40°, in accordance with recent Galileo magnetometer data that indicate the presence of an intrinsic magnetic field such that Jovian magnetic field lines are linked to the surface of Ganymede only at high latitudes. Both the brightness and relative north-south intensity of the emissions varied considerably over the four contiguous orbits (5.5 hours) of observation, presumably due to the changing Jovian plasma environment at Ganymede. However, the observed longitudinal non-uniformity in the emission brightness at high latitudes, particularly in the southern hemisphere, and the lack of pronounced limb brightening near the poles are difficult to understand with current models. In addition to observed solar H I Lyman- α reflected from the disk, extended Lyman- α emission resonantly scattered from a hydrogen exosphere is detected out to beyond two Ganymede radii from the limb, and its brightness is consistent with the Galileo UVS measurements of Barth et al. (1997).

Subject headings: atomic processes — line: identification — planets and satellites:individual (Ganymede, Jupiter) — ultraviolet: spectra

1. INTRODUCTION

Recent observations from both the Galileo spacecraft and the Hubble Space Telescope (HST) have considerably altered our knowledge of the atmospheres of the Jovian satellites Europa and Ganymede. Both are now known to have tenuous atmospheres (column density $\sim 5 \times 10^{14} \text{ cm}^{-2}$) with both molecular oxygen (Europa and Ganymede) and atomic hydrogen (Ganymede) components. The Galileo UV spectrometer detected H I Lyman- α emission at Ganymede from a hydrogen exosphere (Barth et al. 1997), and charged particle measurements indicated that there is also an outflow of protons, implying ongoing gas production (Frank et al. 1997). The oxygen component was detected through HST/Goddard High Resolution Spectrograph (GHRS) observations of the atomic oxygen multiplets O I λ 1304 and O I] λ 1356 (Hall et al. 1995, 1998). The intensity ratio of these emissions implies that the primary source is electron dissociative excitation of molecular oxygen. The source of both the hydrogen and O₂ is thought to be sputtering of surface water ice by Io plasma torus ions. Beyond the fact that they exist, very little is known about these atmospheres, including their vertical structure, areal coverage, and variability, which could be significant if the dominant source is surface sputtering because of the asymmetric nature of the plasma bombardment. Plasma bombardment of the surface is also supported by the recent detection of ozone and O₂ embedded

in the surface ice of Ganymede, and SO₂ embedded in the surface ice of Europa (Spencer et al. 1995; Calvin et al. 1996; Noll et al. 1995, 1996).

Galileo magnetometer measurements have also shown strong perturbations in the Jovian magnetic field near Ganymede (Kivelson et al. 1996, 1997). The measured perturbations indicate that the satellite possesses a magnetic field sufficiently strong ($\sim 1500 \text{ nT}$) to overpower Jupiter's ambient field, and that Ganymede's magnetic and spin axes are roughly aligned (Kivelson et al. 1996). Near Ganymede closest approach the plasma wave experiment also detected a significant population of trapped, charged particles (Gurnett et al. 1996), implying that Ganymede possesses a "magnetosphere within a magnetosphere." Consistent with these results, the HST/GHRS observations (Hall et al. 1998) have raised the intriguing possibility that Ganymede exhibits polar aurora. In those spectra the Ganymede O I] λ 1356 emission line exhibits a doubly-peaked profile that is inconsistent with that of a diffuse source filling the aperture, or with emission from a uniform disk. Hall et al. postulated that the double-peaked profile implies the existence of a similarly double-peaked structure in the spatial distribution of the emission source within the aperture, with the strongest emissions coincident with Ganymede's north and south polar regions. In this paper, we report ultraviolet objective grating images of Ganymede made with the Space Telescope Imaging Spectrograph (STIS) (installed in HST in Febru-

¹Department of Physics and Astronomy, The Johns Hopkins University, Baltimore, Maryland

²Space Telescope Science Institute, Baltimore, Maryland

³Department of Earth and Planetary Sciences, The Johns Hopkins University, Baltimore, Maryland

ary 1997) which confirm the spatial distribution inferred from the earlier observation and raise new questions about the interaction of Ganymede’s atmosphere with the Jovian magnetosphere.

2. OBSERVATIONS

Observations were obtained over four contiguous HST orbits on 1998 October 30 with the STIS G140L grating using the $2'' \times 25''$ slit. At the time of observation, Ganymede was 4.25 AU from Earth, its sub-Earth longitude varied from 290 to 300° and the phase angle was 8.6°. Since the diameter of Ganymede’s disk was $1.''71$, this provided effective objective grating spectroscopy over the wavelength range of 1160 – 1720 Å. A log of the exposures is given in Table 1. The STIS mode used for the observations is the same as that used to observe Io, and the details can be found in Roesler et al. (1999). Two distinct time-tagged spectral images are obtained in each of four HST orbits. The first image in orbits 2–4 exhibits a very high geocoronal Lyman- α background (typically 15 kR as opposed to 3.5 kR during the dark part of an HST orbit) as well as strong O I $\lambda 1304$ airglow emission due to the illumination of the Earth’s upper atmosphere by sunlight. An example of a raw spectral image is shown in Figure 1. Note the $2''$ wide vertical stripe corresponding to geocoronal Lyman- α with the disk reflected Lyman- α image of Ganymede perfectly centered in in the slit. The raw image also shows the two oxygen multiplets, clearly separated, and reflected sunlight at the longer wavelengths.

3. DISCUSSION

3.1. Spectra

Individual spectra (two per orbit) were extracted by summing the data over 82 pixels ($2''$) along the slit centered on Ganymede. The background, particularly the geocoronal Lyman- α , was obtained by summing 151 pixels ($3.''68$) along the slit on both sides of Ganymede, and averaging the two. The results for a single spectral image, with the background subtracted, are shown in Figure 2. In this figure, the one-dimensional extracted spectrum has also been rebinned by four pixels to enhance the signal/noise ratio. The unusual shape of the spectral lines of H I Lyman- α and the two O I emissions result from the spatial distribution of these emissions on the disk of Ganymede.

Longward of 1380 Å the signal is reflected solar radiation. To model this component, a solar spectrum taken with the SOLSTICE instrument on UARS (Woods et al. 1996) appropriate to the level of solar activity in October 1998 was convolved with an assumed uniform reflecting disk of Ganymede’s radius (note that one pixel is $0.''0244 \times 0.''0244$ and the dispersion is $0.584 \text{ \AA pixel}^{-1}$). This is overplotted in Fig. 2. From this fit, the planetary albedo can be derived from the ratio of the reflected flux to the solar flux at Jupiter:

$$p(\lambda) = \frac{F_G(\lambda)\pi d^2}{F_\odot(\lambda)\Omega_G}\phi(\theta, \lambda)$$

where d is the Sun-Jupiter distance (in AU), Ω_G is the solid angle of Ganymede as seen from Earth, $F_\odot(\lambda)$ is the solar flux at 1 AU, and $\phi(\theta, \lambda)$ is the phase function at phase angle θ . To determine the albedo at a wavelength

as close as possible to the oxygen emissions, we choose a 50 Å band centered at 1405 Å. With the assumption of unity for $\phi(\theta, \lambda)$, the derived albedo near 1400 Å is found to be $2.3 \pm 0.2\%$, in good agreement with the value of $2.6 \pm 0.3\%$ derived by Hall et al. (1998) from GHRM measurements of the reflected C II $\lambda 1335$ multiplet. Note that the measurement of Hall et al. was made at a slightly smaller phase angle, 2.7°.

The lower panel of Fig. 2 shows a single spectrum after subtraction of the fitted solar spectrum assuming a constant albedo with wavelength. The two O I emissions are clearly separated and both have a shape determined by the spatial distribution on the disk, similar to that inferred by Hall et al. (1998) from their one-dimensional spectra. The fluxes of the two multiplets are extracted and tabulated, together with the ratio of the two (O I] $\lambda 1356$ /O I $\lambda 1304$), in Table 1. The values are generally consistent with those reported by Hall et al. (note that Hall et al. give the total O I $\lambda 1304$ flux, airglow plus reflected solar radiation), but the orbit to orbit variation suggests a real variability, one that is correlated with the changes in the morphology of the emissions discussed in the next section. The ratio of O I] $\lambda 1356$ to O I $\lambda 1304$ is, like that found by Hall et al., consistently lower (but within the 3σ uncertainty) than the values expected for electron impact excitation of O₂ alone, 1.6–2.0, indicating a possible contribution from electron impact of atomic oxygen to the O I $\lambda 1304$ emission. However, this is not quantifiable as there is an indication, from Fig. 2, that the albedo is increasing below 1300 Å in which case the O I $\lambda 1304$ flux would be over-estimated and the true intensity ratio would be closer to the known value for O₂ excitation.

3.2. O I] $\lambda 1356$ Images

Images of O I] $\lambda 1356$ were constructed using the flat-fielded counts (“ft”) files from the HST pipeline rather than the fluxed two-dimensional image (“x2d”) files used to generate Fig. 1. This was done to avoid distortion introduced by the changing sensitivity across the $2''$ wide slit, which spans 47 Å. To allow for temporal variability, the two separate exposures from each orbit were added together since the O I] $\lambda 1356$ emission is not affected by the higher Lyman- α or O I $\lambda 1304$ background levels. Detector background was evaluated away from Ganymede along the slit and subtracted from the resulting 82×82 pixel array. Each image was then rotated to align Jovian north along the vertical axis, rebinned to 41×41 pixels (each pixel now $0.''049$ on a side), and smoothed by 3 in both directions. The results are shown in Figure 3, together with brightness contours calibrated in rayleighs. The images are characterized by bright polar regions and appear to be variable with time.

The location of the emissions, mostly at geographic latitudes above $|40|^\circ$ in both hemispheres, is in agreement with the model of Kivelson et al. (1997) that predicts the presence of Jovian field lines linked to Ganymede only at high latitudes. In addition, the regions of brightest emission occur at the geomagnetic latitudes where the separatrix regions intersect the atmosphere and which define the boundaries of the polar caps (Neubauer 1998). Magnetic field line reconnection occurs along the separatrix imparting an atmospheric signature of enhanced conduc-

tivity and current known as the auroral or polar electrojets. Over the course of the four orbits the orientation of the Jovian magnetic field relative to Ganymede’s magnetic field, which is tilted 10° from the spin axis (Kivelson et al. 1997), varied considerably, as indicated in Table 1. Thus, the locations of the polar caps and separatrix regions on the surface of Ganymede vary considerably over a Jovian rotation. This can account for both the variations in total O I flux and the relative brightnesses of the northern and southern hemisphere emissions.

However, there are two surprising aspects to these images, because Jovian magnetospheric electrons have direct access to the polar cap atmospheres, as implied by particle and fields measurements on Galileo (Williams et al. 1998; Paranicas et al. 1999). They are the longitudinal non-uniformity in the emission brightness at high latitudes, particularly in the southern hemisphere, and the lack of pronounced limb brightening near the poles, even at the smoothed 200 km spatial resolution of our images. The images yield ~ 50 R limb intensity above the polar caps. Under uniform conditions this is equivalent to ~ 15 R at 60° latitude and below our detection limit. The brightest regions on the disk are 20 times the disk intensity constrained by the observed limb intensity.

To explore the significance of the observed oxygen brightness, a model atmosphere was constructed with surface O_2 density of $1 \times 10^8 \text{ cm}^{-3}$ and column density of $5.2 \times 10^{14} \text{ cm}^{-2}$, which is consistent with the range adopted by Hall et al. (1998) and at the abundance upper limit deduced from a UV stellar occultation observed by Voyager (Broadfoot et al. 1981). For the electron density, a model was generated from measurements by the Galileo plasma wave instrument along fly-by trajectories and extrapolated to the surface with density of 370 cm^{-3} (Gurnett et al. 1996). Unfortunately, there are no observational constraints on the electron temperature. From the data of Sittler & Strobel (1987) at their maximum L shell of 13, one would expect the Jovian magnetospheric electron temperature to be at least 20 eV. For a ~ 9 eV multiplet, the excitation rate would be insensitive to this or higher electron temperatures. With the above assumptions at $T_e \sim 20$ eV applied to the polar atmosphere on open field lines, electron impact dissociative excitation of O_2 yields 300 R of O I] $\lambda 1356$ at high latitudes with limb brightening to ~ 1 kR. A polar limb intensity of 50 R implies an O_2 column density of $3 \times 10^{13} \text{ cm}^{-2}$. Alternatively, in the absence of a direct measurement of Jovian electron temperature, the upper limit column density of $5.2 \times 10^{14} \text{ cm}^{-2}$ is permissible, if $T_e \sim 4$ eV. Also possible would be various combinations of O_2 column density in the range of $(0.3 - 5) \times 10^{14} \text{ cm}^{-2}$ and electron temperature in the range of 4–20 eV or higher.

There are additional factors to consider in the interpretation of the HST images. There is no evidence that Ganymede’s surface temperature drops to the O_2 condensation temperature of 80 K which could account for an inhomogeneous atmosphere. In the range $T_e = 1 - 100$ eV, the calculated intensity ratio of O I] $\lambda 1356$ to O I] $\lambda 1304$ is limited to 1.6–2.0 for a pure O_2 atmosphere. Lower values require the addition of atomic oxygen. In the limit of a pure atomic oxygen atmosphere, this intensity ratio has a value of 1.2 at $T_e = 4$ eV, monotonically decreasing

to ~ 0.35 at 20 eV. There is no apparent correlation of this ratio in Table 1 with absolute O I] $\lambda 1356$ brightness. Clearly to achieve the higher observed ratios requires an O_2 atmosphere. Finally, Jovian magnetospheric electrons on open field lines do not have large density variability on the length scales characteristic of the brightness variations in Fig. 3 (Gurnett et al. 1996).

Thus, the best explanation for the inhomogeneity in the emission brightness is that it is truly auroral in nature, analogous with the Earth’s highly variable UV luminosity in the auroral oval regions and driven by acceleration processes of electrons trapped within Ganymede’s magnetosphere near the separatrix regions. Without knowledge of the distribution function of these auroral precipitating electrons and associated fluxes, the column density of Ganymede’s atmosphere cannot be inferred from the bright auroral regions in HST images. For the present time the polar limb intensities are the only constraint on the atmospheric column density and until the temperature of electrons on open field lines is determined, this constraint is not firm.

3.3. H I Lyman- α

Barth et al. (1997) have reported the detection of H I Lyman- α emission above the limb of Ganymede extending nearly one Ganymede radius (2634 km), which they attribute to a hydrogen exosphere. Such emission should be detectable in our long-slit spectral image but is masked by the strong geocoronal Lyman- α emission that fills the entire $2''$ wide slit (see Figure 1). To remove the geocoronal component, a Lyman- α “flat field” along the slit is needed. This is obtained from our data in the following manner. The final three orbits contain separate spectral images with distinctly different values of geocoronal background, 15 kR for the first of each pair, 3.5 kR for the second. The three “high” images and the three “low” images are separately combined (again using the flat-fielded counts files rather than the flux calibrated files), and spatial profiles along the slit (summing 82 pixels in the dispersion direction) are obtained. These are shown in the top panel of Figure 4. The profiles are normalized to the slightly different cumulative exposure times and the difference is taken, which eliminates the signal due to Ganymede, and this is also shown (after median filtering) in the figure. The geocoronal background is then normalized to and subtracted from the “low” image giving the net Lyman- α spatial profile associated with Ganymede, as shown in the lower panel of Figure 4, where emission above both limbs is clearly detected. The radial model of Barth et al. (1997), integrated across the width of the STIS slit, is also shown in the figure and is found to fit our data very well.

4. CONCLUSIONS

Objective grating images of Ganymede obtained with HST/STIS show clearly separated O I emissions confirming the result of Hall et al. (1998) that the emissions are confined to polar regions (latitudes above 45°). The total fluxes are consistent with those reported by Hall et al. but appear to vary in time and in the relative intensities between northern and southern hemispheres. The O I] $\lambda 1356$ /O I] $\lambda 1304$ ratio is consistent with the primary excitation mechanism being electron impact on O_2 , as postulated by Hall et al. While the spatial distribution of the

emissions is consistent with current models of the magnetic field of Ganymede, expected longitudinal uniformity and limb brightening are not observed. In addition, Lyman- α limb emission from a hydrogen exosphere is detected and the measured brightness is found to be in good agreement with the Galileo UVS observations of Barth et al. (1997).

This work is based on observations with the National

Aeronautics and Space Administration – European Space Agency HST obtained at the Space Telescope Science Institute, which is operated by the Association of Universities for Research in Astronomy, Incorporated, under NASA contract NAS5-26555. We acknowledge partial support by NASA contract NAS5-30403 to the Johns Hopkins University.

REFERENCES

- Barth, C. A., et al. 1997, *Geophys. Res. Lett.*, 24, 2147
 Broadfoot, A. L., et al. 1981, *J. Geophys. Res.*, 86, 8259
 Calvin, W. H., Johnson, R. E., & Spencer, J. R. 1996, *Geophys. Res. Lett.*, 23, 673
 Frank, L. A., et al. 1997, *Geophys. Res. Lett.*, 24, 2152
 Gurnett, D. A., Kurth, W. S., Roux, A., Bolton, S. J., & Kennel, C. F. 1996, *Nature*, 384, 535
 Hall, D. T., Strobel, D. F., Feldman, P. D., McGrath, M. A., & Weaver, H. A. 1995, *Nature*, 373, 677
 Hall, D. T., Feldman, P. D., McGrath, M. A., & Strobel, D. F. 1998, *ApJ*, 499, 475
 Kivelson, M. G., et al. 1996, *Nature*, 384, 537
 Kivelson, M. G., et al. 1997, *Geophys. Res. Lett.*, 24, 2155
 Kliore, A. J., Hinson, F. M., Flasar, F. M., Nagy, A. F., & Cravens, T. E. 1997, *Science*, 277, 355
 Neubauer, F. M. 1998, *J. Geophys. Res.*, 103, 19843
 Noll, K. S., et al. 1995, *J. Geophys. Res.*, 100, 19057
 Noll, K. S., et al. 1996, *Science*, 273, 341
 Paranicas, C., et al. 1999, *J. Geophys. Res.*, 17, 459
 Roesler, F. L., et al. 1999, *Science*, 283, 353
 Saur, J., Strobel, D. F., & Neubauer, F. M. 1998, *J. Geophys. Res.*, 103, 19947
 Sittler, E. C., Jr. & Strobel, D. F. 1987, *J. Geophys. Res.*, 92, 5741
 Spencer, J. R., Calvin, W. M., & Person, M. J. 1995, *J. Geophys. Res.*, 100, 19049
 Williams, D., Mauk, B., & McEntire, R. W. 1998, *J. Geophys. Res.*, 103, 17523
 Woods, T. N., et al. 1996, *J. Geophys. Res.*, 101, 9541

TABLE 1
 IMAGE PARAMETERS AND DERIVED FLUXES

Exposure ID	Start Time (UT)	Exposure Time (s)	O I λ 1304 Flux ^a	O I] λ 1356 Flux ^a	Ratio λ 1356/ λ 1304	Projected Angle of B_J ^b
O53K01010	8:21:19	850.0	12.5 ± 2.1	19.5 ± 2.3	1.6 ± 0.3	17.1
O53K01020	8:38:57	850.0	11.5 ± 2.0	25.1 ± 2.3	2.2 ± 0.4	15.8
O53K01030	9:40:09	1205.0	14.5 ± 5.3	22.5 ± 2.2	1.5 ± 0.6	7.8
O53K01040	10:07:22	1205.0	10.4 ± 1.8	17.5 ± 2.0	1.7 ± 0.3	3.3
O53K01050	11:16:55	1125.0	11.6 ± 5.7	37.7 ± 2.7	3.2 ± 1.6	-8.2
O53K01060	11:42:48	1100.0	20.5 ± 2.2	30.4 ± 2.4	1.5 ± 0.2	-11.6
O53K01070	12:53:42	1200.0	22.1 ± 5.6	26.1 ± 2.6	1.2 ± 0.3	-17.0
O53K01080	13:17:10	1130.0	16.5 ± 2.3	20.2 ± 2.4	1.2 ± 0.2	-17.2

^a 10^{-5} photons $\text{cm}^{-2} \text{s}^{-1}$. Quoted errors are 1σ statistical uncertainty.

^bin degrees measured east of Jovian north (south pole).

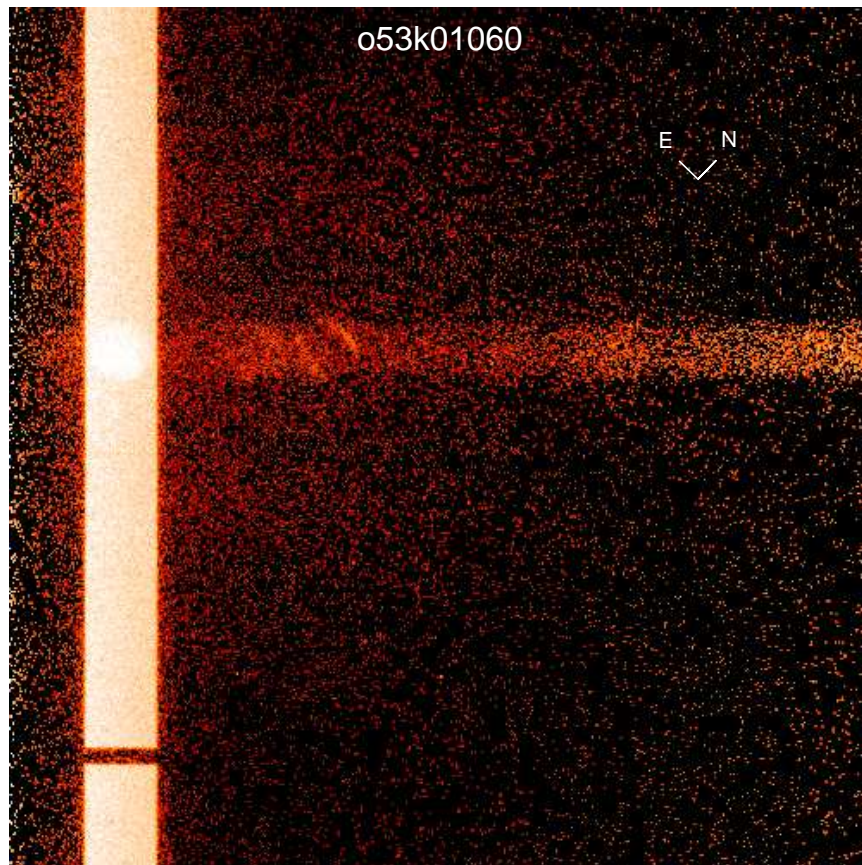


FIG. 1.— An example of a single spectral image (ID o53k01060). The horizontal axis is wavelength, extending from 1150 to 1720 Å, while the height of the image is 25". Jovian north is indicated. The vertical stripe on the left is geocoronal Lyman- α emission.

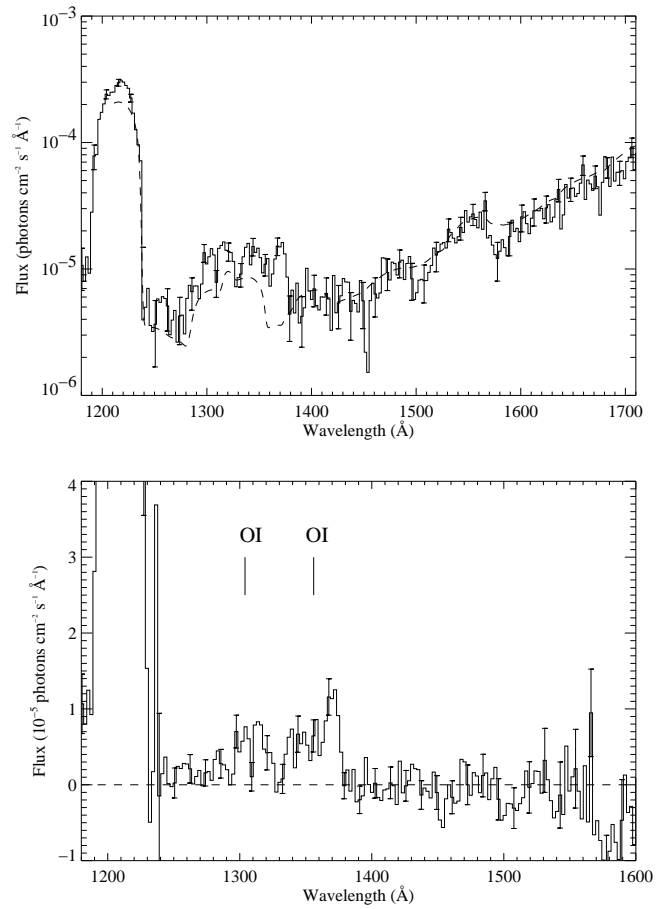


FIG. 2.— Top: Extracted spectrum obtained by summing over the image of Ganymede in Fig. 1. A solar spectrum, convolved with a uniform disk of Ganymede’s diameter, is shown as the dashed curve. Bottom: Difference spectrum obtained by subtracting the fitted solar spectrum. The positions of the O I emissions at the center of the disk are indicated.

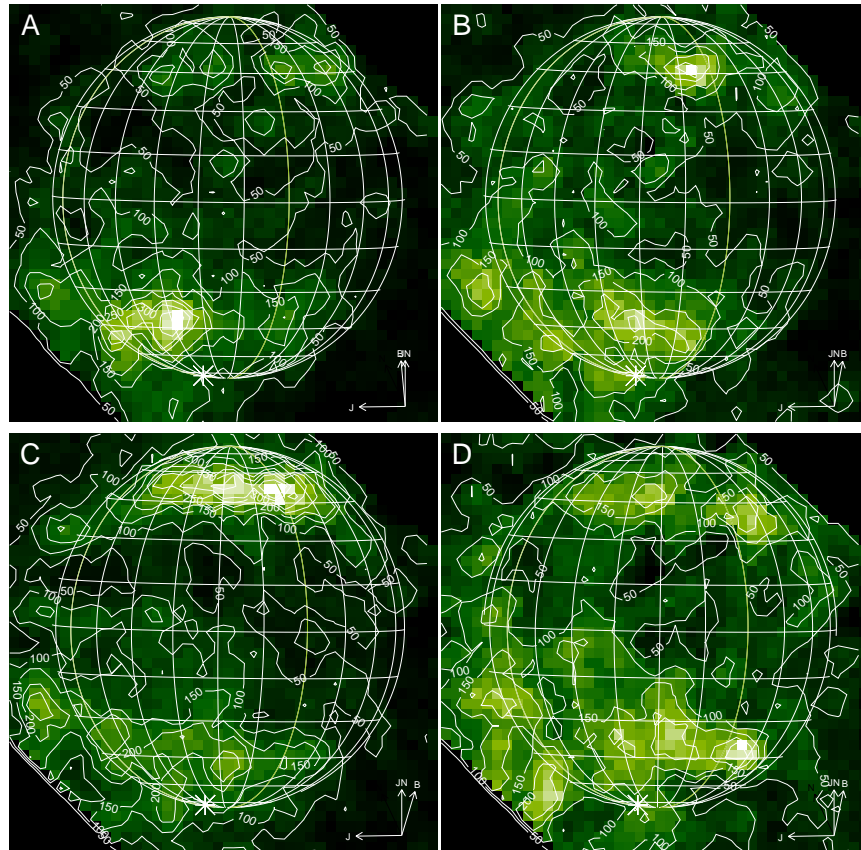


FIG. 3.— Images of O I $\lambda 1356$ emission for each orbit (indicated by A–D) are shown, together with brightness contours in rayleighs. The compass shows Jovian north (JN), the direction to Jupiter (J) and the anti-direction of the Jovian magnetic field (B).

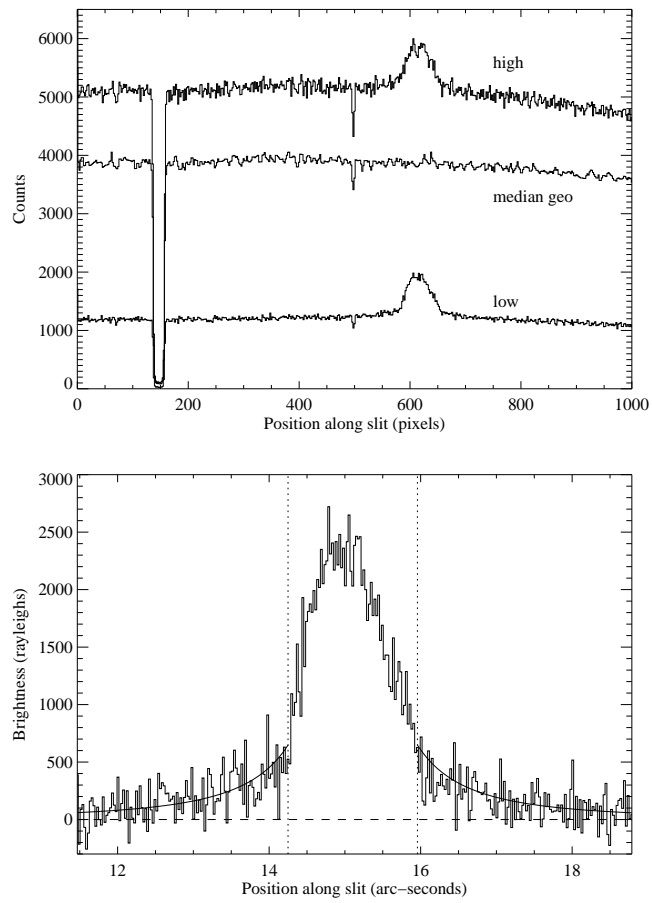


FIG. 4.— Top: Spatial profiles of Lyman- α along the slit. “High” and “low” refer to the first and second exposures, respectively, of orbits 2–4. “Median geo” is the difference smoothed with a 5-point median filter. Bottom: Spatial profile of Lyman- α associated with Ganymede obtained by subtracting the derived geocoronal background. The model of Barth et al. (1997) based on fitting Galileo UVS data is shown.